# Stochasticity of infectious outbreaks and consequences for optimal interventions

Roberto Morán-Tovar<sup>1</sup>, Henning Gruell<sup>2</sup>, Florian Klein<sup>2</sup>, and Michael Lässig<sup>1</sup>

<sup>1</sup>Institute for Biological Physics, Universität zu Köln, Köln, Germany. <sup>2</sup>Laboratory of Experimental Immunology, Institute of Virology, Faculty of Medicine and University Hospital Cologne, Universität zu Köln, Köln , Germany.

#### Abstract

Global strategies to contain a pandemic, such as social distancing and protective measures, are designed to reduce the overall transmission rate between individuals. Despite such measures, essential institutions, including hospitals, schools, and food producing plants, remain focal points of local outbreaks. Here we develop a model for the stochastic outbreak dynamics in such local communities. We derive analytical expressions for the probability of containment of the outbreak, which is complementary to the probability of seeding a deterministically growing epidemic. This probability depends on the statistics of the intra-community contact network and the initial conditions, in particular, on the contact degree of patient zero. Based on this model, we suggest surveillance protocols by which individuals are tested proportionally to their degree in the contact network. We characterize the efficacy of contact-based protocols as a function of the epidemiological and the contact network parameters, and show numerically that such protocols outperform random testing.

The current SARS-CoV-2 pandemic caused millions of deaths and severely affected the global population with multiple consequences for health and economy [1]. Before population-wide immunity is achieved, non-pharmaceutical interventions (NPIs) are required to suppress or mitigate the transmission of the infections [2, 3, 4]. Some measures can easily be implemented and cause only a small burden for the population, such as the usage of protective masks or contact tracing strategies. Other measures such as massive testing, lockdowns and social distancing, can be costly and of large impact for the population [5]. Core institutions such as hospitals, schools, and food supply and producing plants must continue functioning in order to satisfy the basic needs of communities [6]. Under these circumstances, NPIs can be combined in order to avoid local outbreaks. On the one hand, protective measures are implemented to reduce the so-called initial effective reproductive number  $R_0$ , i.e., the average number of new infections caused by an infected individual during its infectious period, slowing down the initial spread of the virus. Additionally, given the high fraction of asymptomatic infected individuals reported for SARS-Cov-2 [7, 8], a surveillance protocol based on regular testing and contact tracing can be performed to detect and control the silent spread of the virus. However, RT-PCR tests can be costly to perform at high coverage even in small populations. Alternative testing strategies, including pool testing [9] and the use of rapid tests, have been developed to tackle this problem. Here we explore surveillance protocols based on random testing of a fraction of the population that can be implemented feasibly. Additionally, we propose strategies to improve such protocols, in order to maximize the probability of detection of infected individuals and to minimize the time before detection and the expected outbreak size.

Recently, different studies have considered strategies of random testing in large and homogeneous populations [10], where the interaction network between individuals is unknown. Other studies have highlighted the importance of the underlying structure of interactions in a population for the implementation of efficient containment strategies [11] and of optimal surveillance protocols to protect patients and healthcare workers [8, 12].

In this study, we present a random testing protocol in the light of epidemiological dynamics, focusing on the role that stochastic effects have on the development of potential outbreaks. We follow the epidemiological nomenclature to distinguish an outbreak and an epidemic [13]: An outbreak consists of a cluster of few infected individuals that can either go extinct due to stochastic fluctuations, or start growing exponentially. In this context, an epidemic corresponds to this last fate, in which the number of infected individuals grows exponentially and take over a large fraction of the population. Here, we study and review some of the most important aspects that define the initial phase of an outbreak and its fate [13, 14, 15, 16]. We work on deterministic and stochastic compartmental models together with a structured population characterized by a network of contacts. In these models, we calculate the initial reproductive number  $R_0$ , which is commonly used to model epidemics and to characterize epidemiological data. We also determine the explicit dependence that the epidemiological dynamics in a network of contacts has on  $R_0$ . Focusing our attention on the different sources of stochasticity, we calculate the extinction probability of an outbreak and study its consequences for the optimal implementation of surveillance strategies. Furthermore, we present a testing strategy of asymptomatic individuals that can be implemented reliably in small populations. Finally, we perform individual-based stochastic simulations of the dynamics of outbreaks on a randomly generated graph that properly recreates a network of social interactions [17]. We explore different ranges of parameters to test the analytical results and properly characterize the system, with special focus on the initial reproductive number. Additionally, we

perform simulations of the surveillance protocol and test its performance numerically. We present a novel connectivity-based protocol that outperforms a protocol based on uniform random sampling of the population.

## Epidemiology of local outbreaks

#### Basic epidemiological model

The most commonly used model in epidemiology is the classical SIR model [18]. It has been used to study the behavior of epidemics because it captures most of the general features of the dynamics and requires few parameters. It consists of a population of individuals, each of which can be susceptible (S), infected (I) or recovered (R). Extensions of the SIR model include other compartments of the population to which individuals can be assigned. In particular, here we consider a compartment of exposed (E) individuals, which are susceptible individuals that got in contact with infected ones but that are not yet able to transmit the infection. This compartment of the population represents infected individuals where the pathogen is in an incubation phase or in a pre-contagious phase. The model is called a SEIR model and its expected dynamics is governed by the following set of differential equations,

$$\dot{S} = -\beta \frac{SI}{N} \tag{1}$$

$$\dot{E} = \beta \frac{SI}{N} - \sigma E \tag{2}$$

$$\dot{I} = \sigma E - \gamma I \tag{3}$$

$$\dot{R} = \gamma I \tag{4}$$

$$\dot{R} = \gamma I \tag{4}$$

We consider a population of constant size N in which susceptible individuals get exposed at a rate proportional to the transmission rate  $\beta$  and the fraction of infected individuals. Exposed individuals move to the infected compartment at a constant rate  $\sigma$ . Infected individuals recover at a constant rate  $\gamma$ . For the case of SARS-CoV-2, we use estimated average pre-contagious period  $(\tau_{\sigma} \equiv \sigma^{-1})$  and infectious period  $(\tau_{\gamma} \equiv \gamma^{-1})$  of 4 days and 6 days, respectively. We choose the parameter  $\beta$  from the interval 0.25-0.75 $days^{-1}$  [1, 19, 20].

### Reproductive number and the relevant time-scale

We are interested in the first stage of the dynamics, where the approximation  $S \approx N$  is valid. In this regime, for the case of a SIR model, the exponential growth rate of the number of infected individuals is given by  $R_0 - 1$  with  $R_0 = \beta/\gamma$  and time is measured in units of  $\tau_{\gamma}$ . This last expression is convenient because the value  $R_0 = 1$  serves as a threshold between epidemic expansion or extinction.

An equivalent expression can be derived for a SEIR model. In this case, the number of both exposed and infected individuals grow exponentially at the same rate,

$$E(t) \sim I(t) \sim e^{(R_0 - 1)t/\bar{\tau}} \tag{5}$$

where the initial reproductive number  $R_0$  of the SEIR model is given by

$$R_0 = \sqrt{1 - 4\frac{\sigma(\gamma - \beta)}{(\sigma + \gamma)^2}},\tag{6}$$

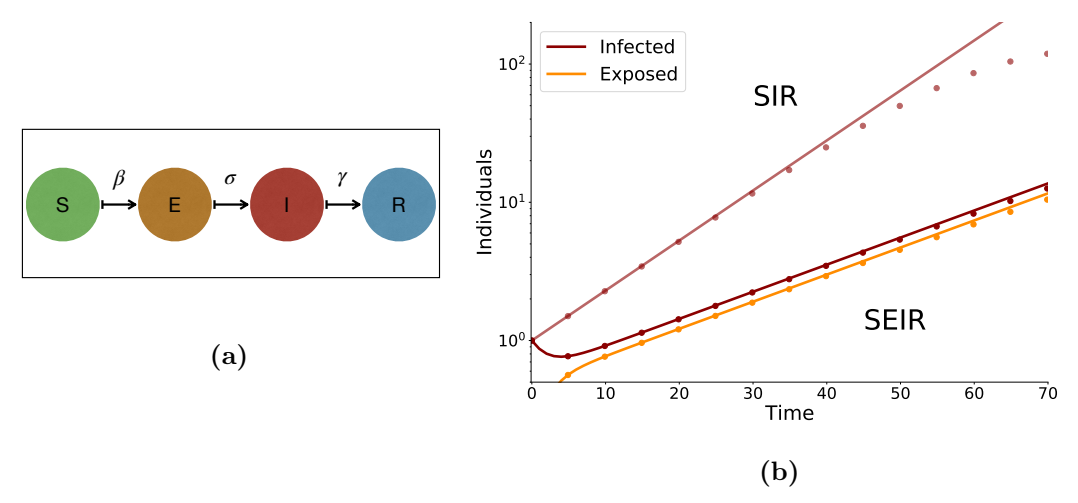


Figure 1. Deterministic dynamics of the SEIR model. (a) We use a 4-compartment model with Susceptible, Exposed, Infected and Recovered individuals. The transition rates between these states,  $\beta$ ,  $\sigma$  and  $\gamma$ , enter the dynamical Eqs. 1- 4. (b) Exposed and Infected individuals follow similar deterministic dynamics. After an initial phase, both subpopulations grow exponentially a rate  $R_0 - 1$  in time units  $\bar{\tau}$ . Solid lines show the analytical solution of Eqs. 1- 4 in the limit  $S \approx N$ . Dots show numerical simulations.

and the time interval  $\bar{\tau}$  is given by the harmonic mean of the pre-contagious and infectious periods,

$$\bar{\tau} = 2 \left( \frac{\tau_{\sigma} \tau_{\gamma}}{\tau_{\sigma} + \tau_{\gamma}} \right). \tag{7}$$

In this case,  $R_0$  is defined as the average number of new exposed/infected individuals produced by a single exposed/infected individual in a time interval  $\bar{\tau}$ . Eq. 5 is commonly used to estimate  $R_0$  from the exponential growth observed in large epidemics. However, the relevant time scale at which the estimated value has a meaning depends on the details of the model. When  $\gamma$  and  $\sigma$  have comparable values, i.e. when the compartment of exposed individuals is required, the time interval  $\bar{\tau}$  properly sets the time scale of the problem rather than  $\tau_{\gamma}$  in order to interpret the value of  $R_0$ .

In addition, the inclusion of the compartment of exposed individuals has another immediate consequence on the dynamics of outbreaks compared to an SIR model. From the deterministic dynamics we learn that, given fixed values of  $\beta$  and  $\gamma$ , the rate of initial exponential growth is reduced (Fig. 1 and Methods). Heuristically, this reduction is caused by the time that each infected individual stays in the exposed state before being able to spread the infection to other individuals.

#### The stochastic fate of an outbreak: epidemic or extinction

Our main interest in this study is the first stage of the dynamics where only few individuals are exposed or infected. Due to low numbers, stochasticity plays an important role affecting both early and late dynamics substantially. For example, a fraction of outbreaks can go extinct before reaching a large number of infected individuals, while some of them eventually infects a large fraction of the population and become an epidemic. Conversely, in outbreaks that become epidemics, the average number of infected individuals grows

faster than the expected deterministic dynamics (see Fig. 2). This initial boost is a posterior effect due to sampling of only trajectories that create epidemics. Moreover, the average time difference at which the deterministic trajectory and stochastic trajectories reach the beginning of the epidemic limit can be several days or few weeks. All these stochastic effects are amplified or weaken depending on the initial reproductive number. For example, for values of  $R_0$  close to 1, the relevant scale at which such effects remain important is large. This can determine drastically the efficiency of control strategies to prevent epidemics.

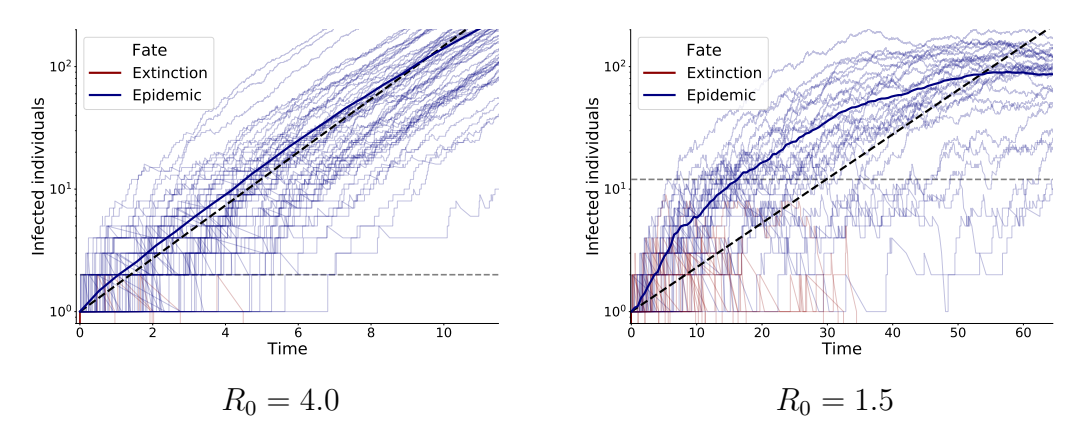


Figure 2. Stochastic dynamics of the SEIR model. Stochastic trajectories of infected individuals in the SEIR model (light solid lines) are shown together with the ensemble average (dark solid lines) and the corresponding deterministic dynamics (black dashed lines). A threshold number of infected individuals (grey horizontal dashed lines), equal to the inverse expected growth rate, separates regimes of strongly stochastic and predominantly deterministic dynamics; see text. We compare high (left) and low (right) initial reproductive numbers to highlight differences in stochasticity of the early dynamics.

To study the stochastic dynamics of the SEIR model we say that, at a given time, each individual n in the populations is in a state  $x_n \in \{s, e, y, r\}$ . The state of each individual at time t + dt, given the state at time t, is governed by the following transition probabilities

$$\mathcal{P}(s \to e) = \beta \frac{I}{N} dt$$

$$\mathcal{P}(e \to y) = \sigma dt$$

$$\mathcal{P}(y \to r) = \gamma dt,$$
(8)
(9)

$$\mathcal{P}(e \to y) = \sigma dt \tag{9}$$

$$\mathcal{P}(y \to r) = \gamma dt, \tag{10}$$

which are defined from the average dynamics of Eqs. 1- 4 and are uniform across individuals.

The probability that an outbreak goes extinct,  $Q_{\text{ext}}$ , depends on different factors such as the initial reproductive number and the current outbreak size. In previous studies [15], it has been derived that  $Q_{\rm ext} = 1/(\beta/\gamma) = 1/R_0$  for an SIR model. A branching process approximation is used, in which the birth and death rates of infected individuals are linear in the limit of  $S \approx N$ . In other words,  $1/R_0$  is the extinction probability of a linear birth-death process where  $R_0$  is the ratio between the birth and the death rates. In this context,  $R_0$  is the expected number of new infections produced by a single infected individual in its recovery period.

As it has been shown above, in the SEIR model exposed and infected individuals

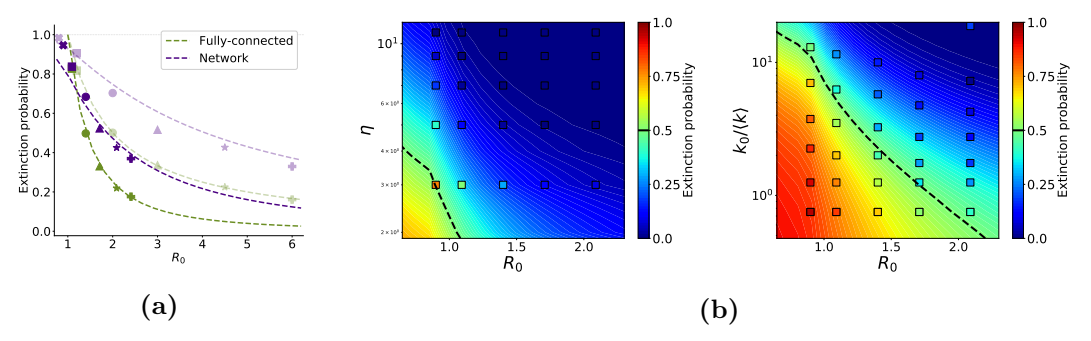


Figure 3. Stochastic fate of an outbreak. (a) Total extinction probability in SIR (transparent) and SEIR (solid) dynamics with (purple) and without (green) a network of contact mediating interactions. Same symbols correspond to equal values of both  $\beta$  and  $\gamma$  in all the curves. (b) Extinction probability as a function of the reproductive number  $R_0$ , the cluster size  $\eta$  (left) and the connectivity of the first infected individual (right). Background represents the analytical prediction and squares show simulation outcomes for various points in parameter space. Black dashed lines delimit when the extinction probability is smaller than the probability of having an epidemic.

grow exponentially at the same rate  $R_0-1$  when the time is rescaled by  $\bar{\tau}$ . In analogy with the SIR model, we can approximate the stochastic SEIR dynamics as a birth-death process of two independent subpopulations of exposed and infected individuals, where  $R_0$  is the expected number of individuals produced within each subpopulation in a time period  $\bar{\tau}$ . In this approximation, the extinction probability of each of the subpopulations is  $1/R_0$  and therefore

$$Q_{\text{ext}} = \left(\frac{1}{R_0}\right)^2. \tag{11}$$

Fig. 3a shows the extinction probability as a function of the initial reproductive number. The probability strongly depends on the type of dynamics: the SEIR model results in a much lower  $Q_{\rm ext}$  than the dynamics from an SIR model at the same  $R_0$ . Note that  $R_0$  is defined differently in the two models. In the case of SEIR, the exposed compartment of the population works as a reservoir of infected individuals. Although these individuals are not yet able to spread the infection further, they will eventually move to the infected compartment without requiring a new contact with an infected individual. Interestingly, as a function of the underlying rates  $\beta$  and  $\gamma$  (same symbols in Fig. 3a), the extinction probability is roughly equal for the two models (solid and transparent lines in Fig. 3a).

#### Stochasticity in the interaction between individuals

In addition to the intrinsic stochasticity of the dynamics due to random events, discreteness and low numbers, other sources of stochasticity and their consequences for the dynamics have been investigated. Most studies have addressed the variability in the initial reproductive number, namely a non-constant  $R_0$  across the population [21], caused by a complex mixture of host, pathogen and environmental factors. Here, we consider an undirected network of contacts that controls the interactions between individuals and translates into an effective variation of infectiousness (Fig. 8b). The structure of contact interactions is characterized by the degree distribution  $\hat{p}(k)$ , which gives the probability that an individual in the network has k contacts with whom it interacts.

Moreover, given that interactions are restricted by the network of contacts, Eqs. 8 is replaced by

 $\mathcal{P}_n(s \to e) = \beta \frac{\sum_{l \in \Omega_n} \delta_{x_l, y}}{k_n} dt, \tag{12}$ 

where  $\Omega_n$  is the set of individuals that interact with individual n and  $k_n$  is the size of  $\Omega_n$ .

In this context, a new variable  $T_{nm}$  has been defined in the literature [13] to characterize the epidemiological dynamics on the network (Methods). It corresponds to the probability of an interaction between individuals n and m that causes a transmission of the infection. We can express the average value of  $T_{nm}$  in terms of the reproductive number,

$$T(R_0) \equiv \langle T_{nm} \rangle = 1 - \left\langle \left( 1 + \frac{R_0}{k^2} \right)^{-1} \right\rangle,$$
 (13)

where  $\langle \cdot \rangle$  denote averages over the degree distribution  $\hat{p}(k)$ . We note that this relation differs from previous work, where an alternative definition of the reproductive number in terms of  $T_{nm}$  has been used [13]. We can use Eq. 13 to infer T from empirical values of  $R_0$  obtained from epidemiological records.

The branching process approximation discussed above is no longer valid for a network of contacts. Given the variable number of neighbors that each individual has, the growth rate of the number of infected individuals is not constant in the population, even in the limit  $S \approx N$ . Similar to Eq. 11, we consider the extinction probability of both infected and exposed individuals, and therefore, the total extinction probability of an outbreak is given by

$$\hat{\mathcal{Q}}_{\text{ext}}(R_0) = \langle \Psi(R_0, k) \rangle \left\langle \langle \Psi(R_0, k-1) \rangle \right\rangle, \tag{14}$$

where  $\langle\langle \cdot \rangle\rangle$  denotes average over the first-neighbor degree distribution  $\hat{p}_2(k) = k\hat{p}(k)/(\sum k\hat{p}(k))$  (See Methods).  $\Psi(R_0, k)$  is the extinction probability of a subpopulation that is seeded in a individual with connectivity k and is given by

$$\Psi(R_0, k) = (1 - T + uT)^k, \tag{15}$$

where u is the solution of a Dyson-like self-consistent equation for the probability that the infection does not spread along the different interacting edges in the network of contacts (See Methods). In Eq. 14, the first brackets corresponds to the total extinction probability of the subpopulation of infected individuals. The second brackets corresponds to the total extinction probability of the subpopulation of exposed individuals. In this last case, the total probability is calculated with an average over the first-neighbor degree distribution because the first exposed infected individual is always a contact of the first infected individual. This first exposed individual has degree k but only k-1 contacts left to spread the infection. A similar expression for the extinction probability in a SIR has been derived before [13].

Fig. 3a shows the extinction probability as a function of the initial reproductive number in the network of contacts. Compared to a fully-connected population, outbreaks have a lower chance of producing epidemics when the interactions are regulated by the network. Moreover, similar to the fully-connected case, the extinction probability is smaller in the SEIR model compared to the SIR model. Finally, when  $\beta$  and  $\gamma$  are kept constant, the extinction probability is roughly the same in the two models. This last point highlights the importance of the right definition of the initial reproductive number when interpreting epidemiological data.

#### Outbreak fate depends on a critical cluster size

As previously discussed, stochastic effects play an important role at the beginning of an outbreak [13, 22, 23, 21]. In particular, there is a non-zero probability that the outbreak goes extinct before it starts to grow exponentially to reach high numbers. This situation is similar to the expansion of a mutant clone under positive selection in an evolving population. In that context, the establishment population size (or equivalently, the corresponding establishment frequency) is defined by the crossover from initial stochastic to predominantly deterministic, exponential growth. On the one hand, a population of size  $\eta$  takes on average  $\eta$  generations to change the number of individuals by  $\eta$  due to stochastic effects. On the other hand, exponential growth changes a population of size  $\eta$  by  $s\eta$  every generation and consequently by  $s\eta^2$  in  $\eta$  generations, where s is the exponential growth rate. Therefore, we expect stochastic effects to be negligible as long as  $s\eta^2 > \eta$ , or  $\eta > 1/s$  [24]. In a fully-connected epidemiological model, the establishment population size of an outbreak is given by  $\eta = 1/(R_0 - 1)$ . However, in the case of a network of contacts, this approximation is no longer valid because each individual has a different effective transmission rate and therefore, the outbreak grows differently depending on the network nodes involved.

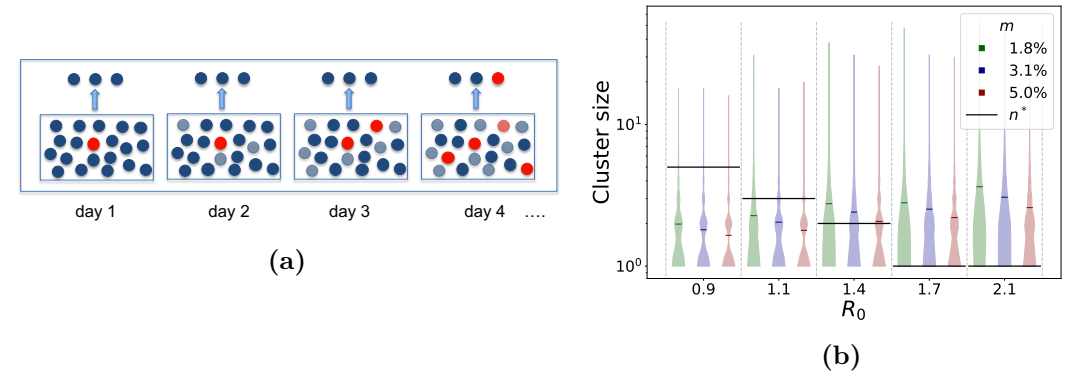


Figure 4. Surveillance random testing protocol. (a) Daily random testing protocol. A constant number of individuals are chosen randomly everyday without replacement. In addition, individuals that are selected, are not replaced in the sampling pool for the next  $\tau_{\sigma}$  days (light blue dots). The outbreak starts with one infected individual (red dots) at day one. (b) Performance of the random testing protocol in terms of the infectious cluster size at the time of a first detection. Black horizontal lines show the establishment threshold.

Here we propose a minimum cluster size that an infectious outbreak should reach before it starts to grow exponentially. More concretely, we say that an outbreak is established whenever the probability of having an epidemic is larger than the extinction probability. Altogether, this suggest that in any surveillance strategy, an outbreak should be detected before it gets established.

To characterize the extinction regime below the establishment threshold, we approximate the extinction probability as a function of the current size of the outbreak  $\eta$  as

$$\hat{\mathcal{Q}}_{\text{ext}}(\eta, R_0) = \langle \langle \Psi(R_0, k-1) \rangle \rangle^{2\eta}. \tag{16}$$

This expression gives the product of extinction probabilities of two subpopulations (infected and exposed) that are seeded in  $\eta$  independent individuals with connectivity k but that only have k-1 contacts left to transmit the infection. This approximation

does not take into account the individual connectivity of the  $\eta$  individuals in each subpopulation, but rather uses the properties of a typical individual that is part of the outbreak.

As expected, the reproductive number  $R_0$  plays an important role. Fig. 3b (left panel) shows the extinction probability as a function of the cluster size and the initial reproductive number. It can be observed that decreasing  $R_0$  increases the extinction probability but also changes the relevant scale at which stochastic effects remain relevant. We define the establishment region as the region where, given  $\eta$  and  $R_0$ ,  $\hat{Q}_{\text{ext}}(n, R_0) < 1/2$ . This condition defines the establishment cluster size function  $\eta^*(R_0)$  (dashed line in Fig. 3b), which we use below to characterize the performance of the surveillance testing protocol.

#### Outbreak fate depends on the networks of contact

To better understand some of the effects of the network of contacts in the dynamics of a potential outbreak as well as in the surveillance protocol, we derive the extinction probability given a fixed connectivity in the network of the first infected individual as

$$\hat{\mathcal{Q}}_{\text{ext}}(k_0, R_0) = \Psi(R_0, k_0) \left\langle \left\langle \Psi(R_0, k) \right\rangle \right\rangle. \tag{17}$$

This expression gives the extinction probability of a subpopulation of infected individuals seeded in an node with connectivity  $k_0$  times the extinction probability of a subpopulation of exposed individuals seeded in an node with connectivity k and averaged over the first-neighbor degree distribution.

Similar expressions to Eqs. 14, 16 and 17 have been derived previously using the idea of percolation in a random network of contacts and a SIR dynamics [13, 14]. The extension to a SEIR dynamics involves two equally growing subpopulations, exposed and infected, both of which must go extinct for the outbreak to end. Moreover, we explicitly relate the probability of an outbreak to the basic reproductive number  $R_0$ , which is straightforward to infer from epidemiological records. In the SEIR model,  $R_0$  depends on the rates  $\beta$ ,  $\gamma$  and  $\sigma$ .

From Eq. 17 and the outcome of the simulations, we observe that the connectivity of the individual where the outbreak starts strongly influences its extinction probability. As expected, highly connected seeding nodes in the network are more likely to produce epidemics than nodes with low connectivity. Fig. 3b (right panel) shows the extinction probability as a function of  $R_0$  and  $k_0$ . For small values of  $R_0$ , a structured population is highly diverse in terms of the likelihood that an individual starts an epidemic. The so-called super-spreader effect is clearly observed here, where most of the local epidemics are seeded in highly connected individuals. Similarly to the establishment cluster size, here we define a critical connectivity regime, where the extinction probability is smaller than the probability of having an epidemic. When the reproductive number is close to 1, only individuals with connectivity  $\approx 10$  times larger than the average connectivity are likely to seed epidemics. Moreover, we see that individuals that have a connectivity smaller than the average connectivity in the population have an extinction probability close to 1 when  $R_0$  is small. Altogether, we observe that some of the information of the contact network is relevant to determine the stochastic fate of an outbreak and that such information can be used to advise surveillance strategies to control epidemics.

## Monitoring protocol for local outbreaks

After characterizing the deterministic and stochastic dynamics of infectious outbreaks, we propose a surveillance strategy based on a daily random testing protocol of a fraction of the total population to detect infected individuals and prevent epidemics. We assume that all the infected individuals are asymptomatic and therefore there is not a way to inform the protocol based on symptoms. In reality, this is not the case. However, at early stages of an outbreak, the number of infected individuals can grow substantially before a first individual, if any, develops symptoms. This also set a minimum performance criterion for the protocol.

We start by considering a simple protocol that consists of a daily uniform sampling of m random asymptomatic individuals from the total population. Individuals that are sampled are then removed from the testing pool for the next  $\tau_{\sigma}$  days (See Fig. 4a). We chose the time period of no replacement because if an individual is tested negative and gets infected on the next day, that individual will not test positive for the next  $\tau_{\sigma}$  days on average. After this period of time, tested individuals are included in the testing pool again.

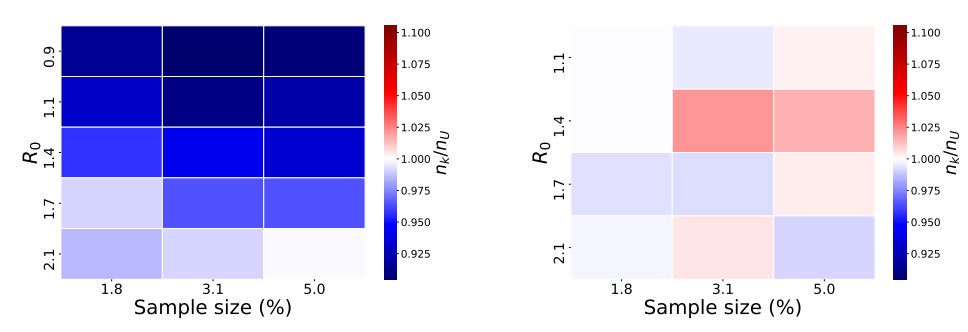


**Figure 5.** Performance degree-based random testing protocol relative to the uniform protocol in terms of cluster size for individuals interacting through a network of contacts (left) and in a fully-connected population (right).

To evaluate the performance of the monitoring protocol, we focus on the average cluster size of infected individuals at the moment of detection and compared with the cluster size establishment limit defined above. Fig. 4b shows that the initial reproductive number is a crucial parameter if we want to detect outbreaks before they are likely to become epidemics. At initial reproductive number close to 1, even with a smallest sampling size consider here (1.8%), the average outbreak size at the first detection is smaller than the establishment size. However, for values of  $R_0 \approx 1.4$ , a sampling size larger than 5% is required to achieve containment. For larger values of  $R_0$ , where the establishment size is 1 individual, other criteria need to be considered to quantify the performance of the surveillance protocol. For example, the time of first detection is crucial to minimize the epidemic size.

#### Efficient monitoring depends on the contact network

As mentioned above, the degree of the seeding node has a big impact on the probability of having an epidemic. Based on that, we calculate normalized likelihood  $L(k_0|\text{epi})$  of

the connectivity of seeding nodes that give rise to an epidemic as follows

$$L(k_0|\text{epi}) = \left(\frac{\hat{p}(k_0|\text{epi})}{\hat{p}(k_0)}\right),\tag{18}$$

where  $\hat{p}(k_0|\text{epi})$  is the degree distribution given that an epidemic has occurred. Using Bayes rule, Eqs. 14 and 17, we upgraded the testing surveillance by using the function L as a weight function for the random sampling of the protocol. Under these conditions, as is shown in Fig. 9, we test highly connected individuals more often than poorly connected ones.

We find an appreciable improvement of the degree-based testing protocol compared to the uniform testing protocol. The performance is better both in the time of detection (See Fig. 10 in Methods) and in the cluster size of the outbreak. Moreover, the improvement is smaller for larger values of  $R_0$ , where the effects of the network are less significant.

Figs. 5 shows the quotient between the cluster size at the moment when the first infected individual is detected in the degree-based sampling protocol,  $n_k$ , and in the uniform sampling protocol,  $n_U$ . The right panel shows that when the population is fully-connected, there is no significant difference between the two protocols. However, when the network of contacts regulates the interactions between individuals, the expected cluster size is reduced in all the range of parameters that we explore. This reduction is greater for smaller values of  $R_0$ , reaching values closed to 10%.

#### Discussion

To prevent large epidemics of infectious diseases, it is important to properly understand the dynamics at early stages of infectious outbreaks. When the average pre-infectious and incubation periods are similar to the average infectious period, it is important to consider a SEIR model rather than an SIR model. The early stage of the outbreak, when  $S \approx N$ , requires an appropriate stochastic description of the dynamics, where extinction and establishment events arise as novel features compared to a deterministic description. The fact that an outbreak can go extinct can be used to set up NPIs under limited by resources or logistic capacity, like the testing protocol presented here. Specifically, the establishment size of an outbreak, as defined above, is a good estimate for the maximum number of infected individuals that can be tolerated before detection of the outbreak.

We have shown that the social connectivity structure in the population plays an important role in the fate of infectious outbreak. The variability of the effective reproductive number introduced by a contact network in the population considerably impacts on the outbreak dynamics. More specifically, a heavy-tailed degree distribution creates a super-spreader effect, where highly connected individuals are more likely to start outbreaks that reach establishment than poorly connected individuals. Although the super-spreader effect has been extensively studied [21, 23, 25, 26, 27], here we dig into some of the concrete causes of its origin, namely the stochasticity of social interactions characterized by the degree distribution of the network of contacts. Moreover, we show that is possible to define, as a function of the initial reproductive number, an upper bound of connectivity for which an individual is not likely to start an outbreak that produces an epidemic.

Finally, based on the contact structure of the population, we show that a degree-based random testing protocol outperforms an uninformed uniform testing protocol (but we do not claim this protocol is optimal in an absolute sense). The difference in

performance depends on the specific parameters of the pandemic spread, which also has important consequences for the overall control of the pandemic worldwide. In practice, the implementation of a degree-based random testing protocol requires a proper estimation of the connectivity of individuals, which can be done by low-cost methods in terms of resources and logistics [28, 29, 30, 31]. Altogether, this shows that understanding the sources of stochasticity and their consequences for the dynamics helps to develop better NPIs to mitigate the adverse consequences of infectious diseases.

### Methods

#### Deterministic dynamics

We use a classical epidemiological model consisting of susceptible (S), exposed (E), infected (I) and recovered (R) individuals. Exposed individuals are infected individuals that do not test positive and cannot infect other individuals yet. The total population size is N.

First, we consider the deterministic dynamics of the system described by the ODE system of Eqs. 1- 4.

We are interested in the first stage of the dynamics, namely, when the approximation  $S \approx N$  is valid. With this approximation, and assuming the initial conditions S(t) = N - 1, E(t) = R(t) = 0 and I(t) = 1, Eqs. 2 and 3 can be written as

$$\dot{E}(t) = -\sigma E + \beta I \tag{19a}$$

$$\dot{I}(t) = \sigma E - \gamma I \tag{19b}$$

The solution of the system of Eqs. 19 is given by

$$\begin{pmatrix} E(t) \\ I(t) \end{pmatrix} = Ce^{\lambda_{+}t} \begin{pmatrix} 1 \\ \frac{\lambda_{+}+\sigma}{\beta} \end{pmatrix} - Ce^{\lambda_{-}t} \begin{pmatrix} 1 \\ \frac{\lambda_{-}+\sigma}{\beta} \end{pmatrix}$$
 (20)

where the constant C is determined by the initial condition and  $\lambda_+$  and  $\lambda_-$  are the eigenvalues of the matrix

$$\begin{pmatrix} -\sigma & \beta \\ \sigma & -\gamma \end{pmatrix}. \tag{21}$$

that are given by

$$\lambda_{\pm} = -\frac{\sigma + \gamma}{2} \pm \frac{1}{1} \sqrt{(\sigma - \gamma)^2 + 4\sigma\beta}.$$
 (22)

As soon as the outbreak is seeded, the time evolution of E and I is lead by the first term in Eq. 20 because  $\lambda_- < 0$  always. With the initial conditions E(0) = 0 and I(0) = 1, Eq. 20 can be written as

$$\begin{pmatrix} E(t) \\ I(t) \end{pmatrix} = \frac{\beta}{\sqrt{(\sigma - \gamma)^2 + 4\sigma\beta}} \begin{pmatrix} 1 \\ \frac{\lambda_+ + \sigma}{\beta} \end{pmatrix} e^{(R_0 - 1) \cdot t/\bar{\tau}} \tag{23}$$

with

$$R_0 = \sqrt{1 - 4\frac{\sigma(\gamma - \beta)}{(\sigma + \gamma)^2}} \tag{24a}$$

$$\bar{\tau} = 2\left(\frac{1}{\tau_{\sigma}} + \frac{1}{\tau_{\gamma}}\right)^{-1} = 2\left(\frac{\tau_{\sigma}\tau_{\gamma}}{\tau_{\sigma} + \tau_{\gamma}}\right) \tag{24b}$$

with  $\tau_{\sigma} = \sigma^{-1}$  and  $\tau_{\gamma} = \gamma^{-1}$ .

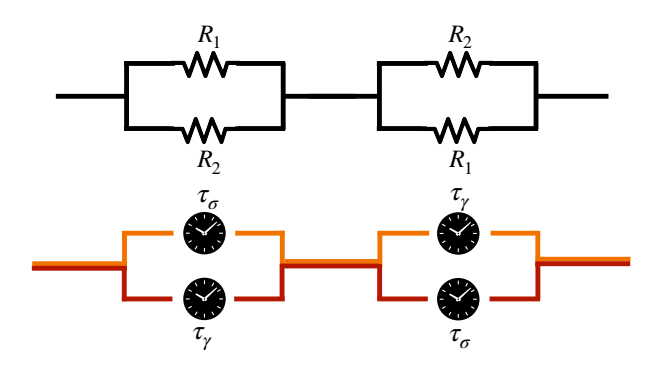
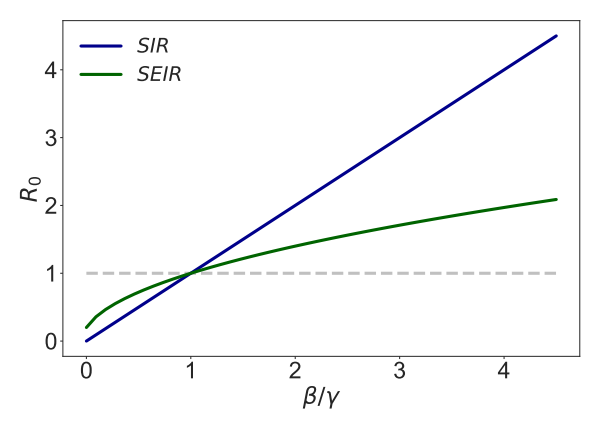


Figure 6. Analogy between a simple electrical circuit and the branching process stochastic model underlying the exponential growth of the number of infected individuals. Resistances correspond to times, currents correspond to average production rate of individuals and voltage across the circuit correspond to the number of new individuals produced in every branching event,  $R_0$ .

The expression of Eq. 24b is analogous to the equivalent resistance of the circuit shown in Fig. 6. To understand the analogy, assume that the  $R_0$ ,  $\tau_{\sigma}$  and  $\tau_{\gamma}$  correspond to  $\Delta V$ ,  $R_1$  and  $R_2$ , respectively. In the case of the circuit, the different currents are adjusted according to Ohms Law to guarantee that the drop in voltage, given the fixed resistances, is  $\Delta V$ . In the case of the birth-death process, the rate of production of individuals (exposed or infected ones) are adjusted to guarantee that the number of new individuals, given the fixed lifetime periods, is  $R_0$ . This analogy can be extended to other nested birth-death processes and can be used to relate the long-term deterministic exponential growth with the underlying stochastic dynamics.

As mentioned above, we decided to include the exposed compartment of the population because it affects dramatically the dynamics of the infected individuals. See Fig. 1. More concretely, for SARS-Cov-2 the estimated average time that takes an exposed individual to become infected  $\tau_{\sigma}$  is in the same order of magnitude of other relevant time-scale, namely the average infectious period  $\tau_{\gamma}$  [1]. Additionally, under these circumstances the classical interpretation of the parameter  $R_0$ , the initial reproductive number, normally defined as the quotient between the infectious rate and the recovery rate  $\frac{\beta}{\gamma}$ , need to be revisited. We derived the expression in Eq. 6 based on the initial exponential growth rate, which in the limit  $\sigma \to \infty$  (exposed individuals turn into infected individuals instantaneously) recovers the  $R_0$  definition.  $R_0$  also indicates whether the infection grows  $(R_0 > 1)$  or shrinks  $(R_0 < 1)$ . However, its interpretation in terms of a branching process is sightly different. It corresponds to the average amount of new exposed/infected individuals produced by a single exposed/infected individual in a time period  $\tau$  given in Eq. 7.

Given the previous definitions, we assume that if measure time in  $\tau$  units, the exposed and infected individuals will grow exponentially with rate  $R_0 - 1$ .



**Figure 7.** Comparison of the initial reproductive number  $R_0$  for the SIR (blue) and the SEIR (green) models.

#### Extinction probability

The extinction probability of an outbreak in an SIR dynamics has been extensively studied. Using a branching process approximation of the stochastic dynamics [15], it has been derived that derived that

$$Q_{\text{ext}} = \frac{1}{R_0},\tag{25}$$

when the outbreak is seeded by a single infected individual. Moreover, given that in a fully-connected SIR model n infected individuals behave as n independent outbreaks of one single infected individual, the extinction probability for an outbreak of size n is given by

$$Q_{\text{ext}} = \left(\frac{1}{R_0}\right)^n. \tag{26}$$

#### **Network Structure**

We generate the random network of contacts by following the Barabasi-Albert method [17]. Such a method produces graphs with heavy-tailed degree distribution  $P_{BA}(k)$ , like the one shown in Fig. 8a. Under these circumstances, most of the individuals have few number of contacts close to the mean degree and a non-negligible amount of individuals have a large number of contacts. The degree of the highly connected individuals can reach values up to two orders of magnitude larger than the mean degree.

In this context, a new variable  $T_{nm}$  has been defined in the literature [13] to characterize the epidemiological dynamics on the random network, which accounts for the average probability that the infection is transmitted through an edge in the network. The average value, T, is given in terms of the typical effective time of duration of an infection  $\tau$ , which is a exponentially distributed stochastic variable, and the rate of infectious encounters between individuals in the network r, such that

$$T_{R_0} \equiv \langle T_{nm} \rangle = 1 - \hat{p}(k) \sum_{k} \int_0^\infty \hat{\rho}(\tau) e^{-t\tau} d\tau$$
 (27)

where the second term correspond to the average probability across the network that no such transmission event occurs. Assuming that r is proportional to  $\beta$  and inversely

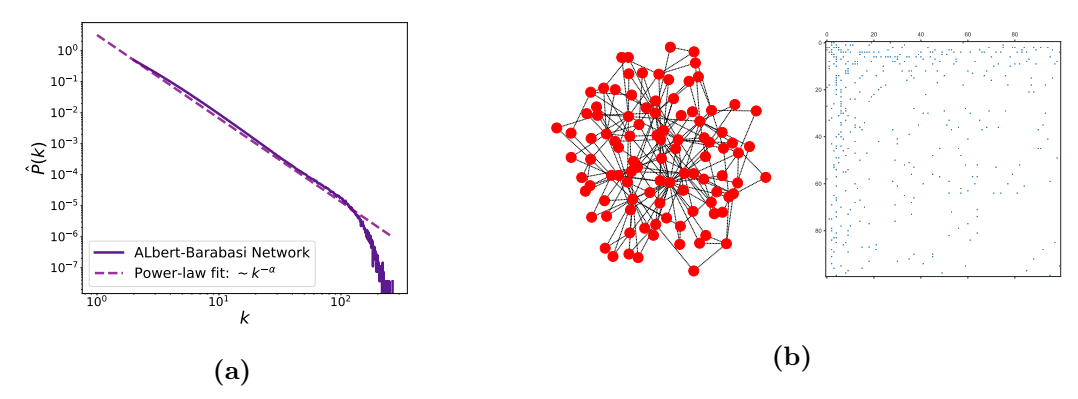


Figure 8. (a) Degree distribution of a random network generated by the Barabasi-Albert method. It characterized by its power-law behavior. (b) Visualization of a random network generated with the Albert-Barabasi scheme together with its adjacency matrix. N=100.

proportional to  $k^2$ , we derived that for the case of a SEIR dynamics, T is given by

$$T = 1 - \sum_{k} \hat{p}(k) \int_{0}^{\infty} e^{\tau} e^{-\frac{R_0}{k^2} \tau} d\tau$$
 (28)

where  $\tau$  is normalized by the mean value  $\bar{\tau}$ .

Moreover, a critical value  $T_c = \langle k \rangle / (\langle k^2 \rangle - \langle k \rangle)$  has been derived for an uncorrelated network previously, which sets the minimum value of T required for an outbreak to have the chance to turn into an epidemic.

We found two important ways in which the stochastic dynamics of the epidemics is affected by the network structure. On one side, the exponential growth rate after establishment finds an earlier saturation presumably produced by boundary effects of the spatially growing infected subpopulation. Additionally, the connectivity of the node where the outbreak starts influences the extinction or epidemic probability of it. We focus our attention of the second observation and derived the probability of an epidemic as a function of the connectivity of the first infected individual,  $k_0$ .

As it has been derived before [13], we start the derivation with a Dyson-like self-consistent equation for the probability u that an individual at the end of a randomly selected interacting edge will produce an epidemic.

$$u = \frac{\sum_{k=1}^{\infty} k\hat{p}(k)\Psi(T, k-1)}{\sum_{k=1}^{\infty} k\hat{p}(k)}.$$
 (29)

where

$$\Psi(T,k) = (1 - T + (Tu))^k \tag{30}$$

and where 1-T is the probability that the disease does not spread through de interacting edge, Tu is the probability that it spreads through the edge but it does not produce an epidemic and  $k\hat{p}(k)/(\sum_k k\hat{p}(k))$  is the distribution of interacting edges connected to an individual at the end of a randomly selected interacting edge. We solved Eq. 29 numerically for a fixed value of T.

Similar equations as Eqs. 16 and 17 are derived in [14] in terms of T for the SIR model. Here, we are able to write them in terms of the epidemiological parameters that define the dynamics of Eqs. 1- 4 and 10 for the case of the SEIR model.

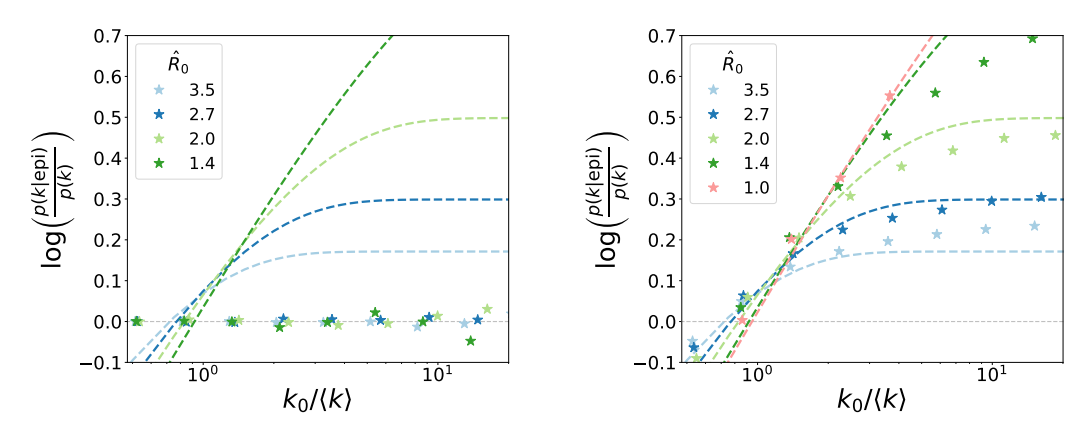


**Figure 9.** Log-likelihood of finding a node in the network with connectivity k given that an outbreak seeded on it produces an epidemic for a fully-connected population (left) and a population that interact with a network of contacts (right).

## Random testing protocols and the Likelihood function

The normalized likelihood function defined in the main text should be reduce to a constant value when the network of contacts is turned off because then  $Q_{\text{ext}|k} = Q_{\text{ext}}$ 

Fig. 10 shows the outcomes of the simulations for the average time of first detection to complement the evaluation of the performance of the degree-based sampling testing protocol. Similar to the cluster size, there is an significant improvement in the time at which the first infected individual is detected. For small values of  $R_0$  the reduction of such time can be large than 10%.

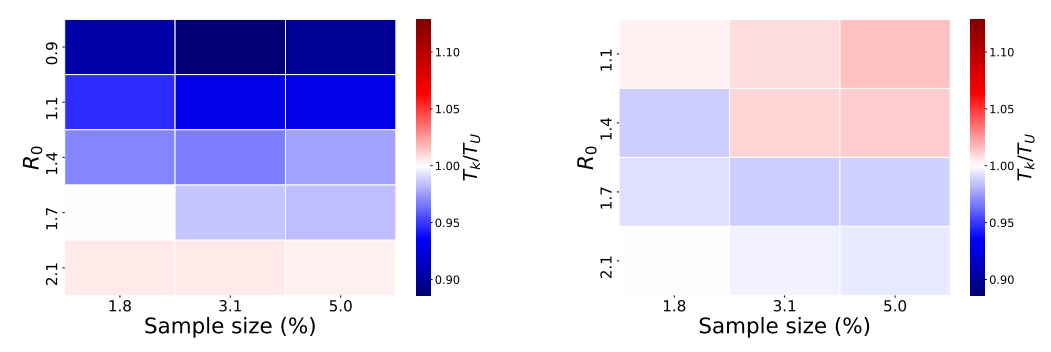


**Figure 10.** Performance degree-based random testing protocol relative to the uniform protocol in terms of time of first detection.

To test that the random testing protocol has an effect on a structured population characterized by a network of contacts, we simulate the degree-based sampling protocol turning off the network of interaction as a negative control but still using the likelihood function L described above for the sampling of individuals. Figs 5 and 10 (right panels) show the performance of the protocol in terms of cluster size and time of the first detection, respectively. In both cases a reduction is achieved, specially when the reproductive number is small and therefore, the effects of the network of contacts become more relevant.

#### Numerical Simulations

The simulations were performed with a modified version of the individual-based SEIR python code seirsplus publicly available in https://github.com/ryansmcgee/seirsplus. The simulations consist of a Gillespie algorithm for independent Poisson processes.

## Acknowledgment

This work has been supported by the Deutsche Forschungsgemeinschaft (DFG) through the Collaborative Research Center 1310, Predictability in Evolution. We want to thank M. Meijers for a careful reading of the manuscript and to R. S. McGee for making available Seirsplus.

#### References

- 1. Y. M. Bar-On *et al.*, *eLife* **9**, ed. by M. B. Eisen, e57309, ISSN: 2050-084X, (https://doi.org/10.7554/eLife.57309) (2020).
- 2. O. Karin *et al.*, "Cyclic exit strategies to suppress COVID-19 and allow economic activity", 2020.
- 3. B. J. Cowling *et al.*, *The Lancet Public Health* **5**, e279–e288, ISSN: 24682667, (http://dx.doi.org/10.1016/S2468-2667(20)30090-6) (2020).
- 4. S. Flaxman et al., Nature 584, 257–261, ISSN: 14764687 (2020).
- 5. P. G. Walker et al., Science **369**, 413–422, ISSN: 10959203 (2020).
- 6. J. R. Black et al., The Lancet **395**, 1418–1420, ISSN: 1474547X (2020).
- 7. R. Li et al., Science (New York, N.Y.) **3221**, 1-9, ISSN: 1095-9203, (http://www.ncbi.nlm.nih.gov/pubmed/32179701) (2020).
- 8. L. Rivett et al., eLife 9, 1–20, ISSN: 2050084X (2020).
- 9. L. Mutesa *et al.*, *Nature* **589**, 276–280, ISSN: 14764687, (http://dx.doi.org/10. 1038/s41586-020-2885-5) (2021).
- M. Müller et al., "Using random testing to manage a safe exit from the COVID-19 lockdown", 2020, arXiv: 2004.04614, (http://arxiv.org/abs/2004.04614% 0Ahttp://dx.doi.org/10.1088/1478-3975/aba6d0).
- 11. J. A. Firth et al., Nature Medicine 26, 1616–1622, ISSN: 1546170X (2020).
- 12. X. Qiu et al., BMJ Open 11, 1–10, ISSN: 20446055 (2021).
- 13. M. E. Newman, Physical Review E Statistical Physics, Plasmas, Fluids, and Related Interdisciplinary Topics 66, 1–11, ISSN: 1063651X (2002).
- 14. L. A. Meyers *et al.*, Journal of Theoretical Biology **232**, 71–81, ISSN: 00225193 (2005).
- 15. L. J. Allen, *Infectious Disease Modelling* **2**, 128-142, ISSN: 24680427, (http://dx.doi.org/10.1016/j.idm.2017.03.001) (2017).
- 16. W. Tritch et al., Infectious Disease Modelling 3, 60-73, ISSN: 24680427, (https://doi.org/10.1016/j.idm.2018.03.002) (2018).

- 17. A.-L. Barabási *et al.*, *Science* **286**, 509-512, ISSN: 0036-8075, (https://science.sciencemag.org/content/286/5439/509) (1999).
- 18. N. Bailey, The Mathematical Theory of Infectious Diseases and Its Applications (Griffin, 1975), ISBN: 9780852642313, (https://books.google.de/books?id=IXtrQgAACAAJ).
- 19. X. He et al., Nature Medicine 26, 672–675, ISSN: 1546170X (2020).
- 20. T. C. Jones *et al.*, *Science* (*New York*, *N.Y.*) **5273**, 1-21, ISSN: 1095-9203, (http://www.ncbi.nlm.nih.gov/pubmed/34035154) (2021).
- 21. J. O. Lloyd-Smith et al., Nature 438, 355–359, ISSN: 14764687 (2005).
- 22. A. Allard *et al.*, "The role of directionality, heterogeneity and correlations in epidemic risk and spread", 2020, arXiv: 2005.11283, (http://arxiv.org/abs/2005.11283).
- 23. B. M. Althouse et al., PLoS Biology 18, 1–13, ISSN: 15457885 (2020).
- 24. M. M. Desai *et al.*, *Genetics* **176**, 1759–1798, ISSN: 00166731, arXiv: 0612016 [q-bio] (2007).
- 25. O. Reich *et al.*, "Modeling COVID-19 on a network: super-spreaders, testing and containment", 2020.
- 26. D. Miller et al., Nature Communications 11, ISSN: 20411723, (http://dx.doi.org/10.1038/s41467-020-19248-0) (2020).
- 27. A. Goyal et al., eLife 10, 1–63, ISSN: 2050084X (2021).
- 28. P. D. Killworth *et al.*, *Social Networks* **12**, 289-312, ISSN: 0378-8733, (https://www.sciencedirect.com/science/article/pii/037887339090012X) (1990).
- 29. H Russell Bernard et al., Social Science Research 20, 109-121, ISSN: 0049-089X, (https://www.sciencedirect.com/science/article/pii/0049089X9190012R) (1991).
- 30. T. H. McCormick et al., Journal of the American Statistical Association 105, PMID: 23729943, 59-70, eprint: https://doi.org/10.1198/jasa.2009.ap08518, (https://doi.org/10.1198/jasa.2009.ap08518) (2010).
- 31. R. Maltiel *et al.*, *The Annals of Applied Statistics* **9**, 1247 -1277, (https://doi.org/10.1214/15-AOAS827) (2015).